

Acidity of Keggin-Type Heteropolycompounds Evaluated by Catalytic Probe Reactions, Sorption Microcalorimetry, and Density Functional Quantum Chemical Calculations

Billy B. Bardin, Shailendra V. Bordawekar, Matthew Neurock, and Robert J. Davis*

Department of Chemical Engineering, University of Virginia, Charlottesville, Virginia 22903

Received: May 22, 1998; In Final Form: October 5, 1998

The acidity and its effects on reactivity of Keggin-type heteropolycompounds were examined by catalytic probe reactions, microcalorimetry of ammonia sorption, and density functional quantum chemical calculations. Phosphotungstic, phosphomolybdic, silicotungstic, and silicomolybdic acids were used as model compounds. The specific rates of double-bond isomerization of both 1-butene and *cis*-2-butene were orders of magnitude greater on the tungsten heteropolyacids than on molybdenum heteropolyacids, which suggests the tungsten-containing solids are stronger acids. The rate of double-bond isomerization over silicotungstic acid was similar to that over phosphotungstic acid, indicating the minor role of the heteroatom. Results from ammonia sorption microcalorimetry showed ΔH_{sorp} on tungsten-based heteropolyacids was approximately 40 kJ mol⁻¹ higher than the corresponding enthalpy obtained on molybdenum-based heteropolyacids. Residual waters of hydration significantly affected both reaction rates and sorption enthalpies. Quantum chemical calculations revealed the most energetically favorable site of the acidic proton to be a bridging oxygen atom in the anhydrous heteropolyacid. Calculations on structurally optimized small metal oxide clusters, as well as the complete Keggin unit, were used to determine the proton affinities by DFT methods. Regardless of cluster size, the proton affinity of a tungsten cluster was always lower than that of an analogous molybdenum cluster by about 20–40 kJ mol⁻¹. The combination of results from experiments and quantum chemical calculations provides a consistent ranking of acid strength for this important class of solid catalysts.

Introduction

The recent push for environmentally friendly chemical processes has led to much research in advanced separations, process integration, and end-of-pipe pollution reduction techniques.¹ Redesign of the basic process cornerstones such as catalysts can also aid in pollution reduction. Since many processes currently use corrosive liquid acids to catalyze reactions, significant opportunities exist for new solid acid catalysts. Therefore, research in developing highly active and selective solid acid catalysts has made great progress in recent years, and many reviews have been written in this area.^{2–7} A recurring problem in the field is the evaluation of density and strength of acid sites on solid surfaces.

Numerous methods have been used to probe solid acidity, but no single technique has proven to be reliable. Common methods for characterizing solid acids include titration with Hammett indicators, temperature-programmed desorption, adsorption microcalorimetry, catalytic probe reactions, and NMR spectroscopy.⁸ In recent years, investigation of model compounds by quantum chemical calculations has also been used to evaluate solid acidity.^{9,10} Since each method has its limitations, a combination of complementary techniques is needed to provide insights into the nature of solid acidity. Some of the advantages and disadvantages of these techniques are discussed below.

Titration with a variety Hammett indicators is one of the most widely used techniques to measure the distribution of acid strengths on solid surfaces.² Unfortunately, if a solid is highly colored, the titration can be very difficult or impossible to perform. The titration method provides only a qualitative measurement of acidity. Interaction of the indicator molecule

with a surface may lead to a stabilization effect which is not accounted for in the Hammett acidity function.⁷ Many arguments have been raised in the past against the use of Hammett indicators for evaluation of solid acidity.^{7,8,11,12}

A second commonly used technique to study solid acids is temperature-programmed desorption (TPD) of adsorbed bases such as ammonia or pyridine. The relative acid strength is inferred from the temperature at which the probe molecule desorbs from the catalyst surface, and the total number of adsorption sites is obtained from the integrated peak intensity. Even though temperature-programmed desorption provides some indication as to the bond strength of probe molecules to surface sites, the technique alone cannot differentiate between Lewis and Brønsted sites. Since ammonia has also been shown to bind strongly to some base catalysts, the choice of the probe molecule is crucial in appropriately characterizing the surface.²

Complementary to TPD, adsorption microcalorimetry involves measuring the heat evolved during the adsorption of various probe molecules on an acidic solid.^{8,13–15} In a single experiment, the total density of adsorption sites and the distribution of adsorption enthalpies can be determined. However, the heats of adsorption of gas-phase molecules on solid acid sites are not only a function of the acid strength of the adsorbent, but also a function of the gas-phase proton affinity of the probe molecule.¹¹ In addition, microcalorimetry cannot differentiate between adsorption on Lewis and Brønsted acid sites.

In addition to the titration-type methods discussed above, catalytic activity can be used to rank solid acidity. Indeed, activity of a catalyst for skeletal isomerization of butane is often used to indicate very strong acidity. Trace olefins in the feed,

however, have been shown to play a considerable role in the rate of isomerization over solid acids and should be rigorously eliminated from reactant streams.^{16–19} Since the mechanism of butane isomerization is sometimes bimolecular,^{16,19} steric hindrance within micropores can also affect catalytic activity.^{19,20} Considering these issues, rates of alkane isomerization alone cannot be used to compare acidities of structurally different compounds.

Advances in solid-state nuclear magnetic resonance (NMR) spectroscopy have enabled site-specific characterization of solid acids such as protonated zeolites.^{21,22} Recently, ranking of solid acid strength by proton NMR spectroscopy has been devised based on the interaction of acid sites with water molecules.²³ In addition, the ¹³C chemical shift of adsorbed probe molecules has been related to the acid strength of the solid.^{2,8,24} One drawback of NMR spectroscopy is the complex interpretation of chemical-shift information due to hydrogen bonding.

The limitations of experimental methods have motivated the use of computational chemistry to describe the fundamental nature of the acid site. For example, the calculated proton affinity (PA) can be used to compare various acidic compounds. The proton affinity is, by definition, the strength of the bond between a proton and a molecule and is calculated as the negative enthalpy of the reaction $A + H^+ \rightarrow AH^+$.²⁵ For small gas-phase molecules such as ammonia or methane, the proton affinity can be determined experimentally using a mass spectral technique.²⁶ Theoretical quantum chemical calculations can be used to compute the proton affinity by specifically adding the proton to a particular site and computing its enthalpy of interaction. Quantum chemically derived proton affinities of small molecules are comparable to those measured experimentally.^{27,28} The measurement of proton affinity of a solid is difficult and involves determination of the affinity distribution at a solid–liquid interface.^{29–31}

The proton affinities of well-ordered solids determined from quantum chemical calculations may provide a relative scale for acid strength. For structurally similar solids, those with the highest proton affinities will likely be the poorest acids. In modeling the acid character of solids, calculations of both proton affinity and binding energy of a probe molecule are ultimately necessary to arrive at a reasonable description of the acid site. Quantum chemical modeling of acid sites in zeolites has been carried out over the last several years,^{9,10,32–36} resulting in a range of values from 1160 to 1374 kJ mol⁻¹ for the proton affinity.⁸ However, to the best of our knowledge, the proton affinities of heteropolyacids have not yet been calculated.

Computer modeling of solid acids also has its limitations. In most cases, the models are idealized approximations of real systems. For example, accounting for the effect of long-range interactions on the acid site becomes difficult without making approximations. Also, the incorporation of solvent effects, e.g., the effect of water on a nearby acid site, is not a trivial task.

One class of solid acids that has broad application in many fields, including catalysis, is heteropolyacids (HPA's). A recent volume of *Chemical Reviews* was dedicated to the many uses of these materials.³⁷ They have long been recognized as exceptional catalysts for a variety of acid-catalyzed reactions,^{38,39} and some processes using HPA's as homogeneous acid catalysts have already been commercialized.^{38–40} A reduced need for separation processes is only one of the several advantages of solid heteropolyacids over liquid acids.

Heteropolyacids are composed of primary, secondary, and tertiary structures. The primary structure is the main building block of the HPA. Many primary structures are known, but the

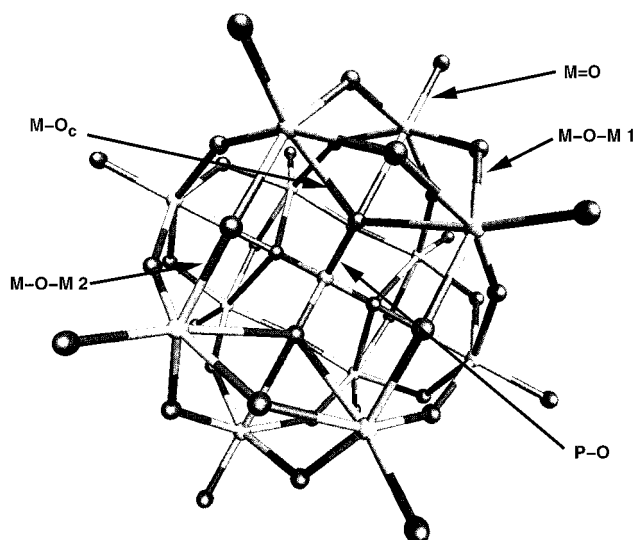


Figure 1. The Keggin structure. M–O_c is the metal–central–oxygen bond. P–O is the central–atom–oxygen bond. M=O is the terminal oxygen–metal bond. M–O–M bonds are bridging metal–oxygen bonds.

most common and thermally stable is the Keggin unit,⁴¹ shown in Figure 1. The Keggin unit consists of a central atom (usually P, Si, or Ge) in a tetrahedral arrangement of oxygen atoms, surrounded by 12 oxygen octahedra containing the addenda atoms (often tungsten or molybdenum). There are four types of oxygen atoms found in the Keggin unit, the central oxygen atoms, two types of bridging oxygen atoms, and terminal oxygen atoms. The secondary structure takes the form of the Bravais lattices, with the Keggin units located at the lattice positions. Heteropolyacids possess waters of crystallization that bind the Keggin units together in the secondary structure by forming water bridges.³⁹ Tertiary structures can be observed when heavy alkali salts are formed.³⁹

The acidity of the heteropolyacid is purely Brønsted in nature. Since the Keggin unit possesses a net negative charge, charge-compensating protons or cations must be present for electro-neutrality. In the hydrated phase, the protons reside in the bridging water moieties forming H₅O₂⁺.³⁸ However, when the HPA has been fully dehydrated, the positions of the protons are not as easily defined. Kozhevnikov et al. concluded from ¹⁷O nuclear magnetic resonance spectroscopy that the most likely position of the proton is on the terminal oxygen.^{42,43} Lee et al. found from infrared spectroscopy that protons were most likely located on the bridging oxygens.⁴⁴ Barrows et al. found from crystallographic analysis that the acidic proton was located on the bridging oxygen for a molybdenum-based heteropolyacid.⁴⁵ Extended Hückel molecular orbital calculations showed the bridging oxygens are the most basic and thus the most likely position for protons to reside.⁴⁶

Evaluation of acid strength in solution has shown that HPA's composed of tungsten are more acidic than those composed of molybdenum, and the effect of the central atom is not as great as that of the addenda atoms. Nevertheless, phosphorus-based heteropolyacids are slightly more acidic than silicon-based heteropolyacids. This gives the general order of acidity as H₃-PW₁₂O₄₀ > H₄SiW₁₂O₄₀ and H₃PW₁₂O₄₀ > H₄PMo₁₂O₄₀.³⁹

The goal of this work is to apply the combination of three methods, catalytic probe reactions, ammonia sorption micro-calorimetry, and quantum chemical calculations, to evaluate the acidity of solid heteropolyacids. In this study, we have examined Keggin-type HPA's: phosphotungstic acid (PW), phosphomolybdic acid (PMo), silicotungstic acid (SiW), and silico-

molybdic acid (SiMo). Double-bond isomerization of 1-butene and *cis*-2-butene were utilized as catalytic probe reactions since the molybdenum-based heteropolyacids showed little activity for butane skeletal isomerization. In addition, the ratio of *trans*-2-butene to 1-butene from a feed of *cis*-2-butene correlates with acidic strength.³ Microcalorimetry of ammonia sorption was also used to rank acid strength. Finally, since heteropolyacids have well-defined local structures, they provide an excellent opportunity for the use of theoretical calculations. First principle quantum chemical calculations were, therefore, used to calculate proton affinities of the various heteropolyacids.

Experimental Methods

Materials. The heteropolyacids H₃PW₁₂O₄₀, H₄SiW₁₂O₄₀, H₃PMo₁₂O₄₀, and H₄SiMo₁₂O₄₀ utilized in these studies were obtained from Aldrich and used without further purification. A cesium salt of phosphotungstic acid was synthesized as described previously.^{19,47} Phosphotungstic acid was dissolved in distilled, deionized water and titrated with an aqueous solution of cesium nitrate (Aldrich). The resulting white precipitate was isolated by evaporation. The cesium salt used here contained two cesium atoms per Keggin unit (Cs₂HPW₁₂O₄₀), since this composition was the most active catalyst for paraffin isomerization.^{19,48}

Characterization. Thermal gravimetric analysis (TGA) of the sample was conducted using a TA Instruments 2050 Thermal Gravimetric Analyzer with helium (BOC Gases, grade 6) flowing at 100 cm³ min⁻¹. The temperature program was a simple linear ramp from 303 to 873 K for PMo and from 303 to 1000 K for PW at a rate of 10 K min⁻¹. Approximately 203.8 or 436.4 mg of sample was used for PMo or PW, respectively.

Surface area measurements (BET) were performed on a Coulter Omnisorp 100CX using dinitrogen (BOC Gases) at 77 K. Surface areas were determined after outgassing at various temperatures (373, 473, 573, and 673 K) to correspond with the pretreatment conditions used in the catalytic studies.

The enthalpy of ammonia sorption on heteropolyacids was measured using a homemade Calvet-type differential heat flow microcalorimeter based on a design described elsewhere.^{49,50} Approximately 0.1 g of sample was placed in the sample cell and evacuated at 473 K for 2 h prior to ammonia sorption. After the cell was cooled to 373 K, ammonia (BOC Gases, anhydrous) was dosed into the cell and the heat flux was recorded. Some samples were also evacuated at higher temperatures (573 and 723 K) to examine the effect of pretreatment conditions.

Catalytic Probe Reactions. Double-bond isomerization of 1-butene was carried out in a single pass, fixed-bed reactor system. The tungsten-based heteropolyacids were diluted in chromatographic silica gel (Fisher) so that very small amounts of catalyst could be loaded into the reactor. Other samples were used without dilution. The catalysts were first pretreated in situ at 373, 473, 573, or 673 K in flowing helium (BOC Gases, Grade 5) at 10 cm³ min⁻¹ for 2 h before catalytic reaction. The fraction of 1-butene (Aldrich) in the feed was 5 vol % in flowing He to give a total flow rate of 30 cm³ min⁻¹. Regardless of pretreatment temperature, the reaction was carried out at 348 K. Products were analyzed by on-line gas chromatography using a HP 5890 II GC equipped with a flame ionization detector and a 50 m, 0.32 mm i.d. alumina/KCl PLOT column.

Double-bond isomerization of *cis*-2-butene was also used as a probe reaction for the catalyst samples and was conducted in accordance with the procedures described above. The catalysts

for this reaction were all pretreated in situ at 473 K in flowing helium (10 cm³ min⁻¹) for 2 h. The reaction was conducted at 348 K.

Computational Methods

Proton affinities of the heteropolyacids were derived from density functional theory (DFT) quantum chemical calculations. These methods have increased in popularity due to the relatively high accuracy of the results compared to the relatively low computational cost. Density functional methods have been shown to predict bond lengths to within about 0.05 Å and bond energies to within about 20 kJ mol⁻¹ for well-defined organometallic systems.^{51,52} In this work, proton affinities were computed by subtracting the energies of the proton and the negatively charged bare cluster from the energy of the optimized protonated complex as shown in eq 1. The geometries and

$$PA = -(E_{H+Cluster} - E_H - E_{Cluster}) \quad (1)$$

energetics for all clusters examined herein were computed using spin-polarized DFT calculations. The electronic structure for each cluster was determined by iterating on the system density to solve the series of single-electron Kohn–Sham equations, thus providing a self-consistent solution. Analytical derivatives are computed during each SCF cycle and used to establish the relative changes in the nuclear coordinates for subsequent geometry optimization steps. All calculations were performed using the Vosko–Wilk–Nusair (VWN) exchange-correlation potential⁵³ with Becke^{54,55} and Perdew⁵⁶ nonlocal gradient corrections for the correlation and exchange energies, respectively. Gradient corrections were included in each iteration of the self-consistent field cycle. The density and energy of each SCF cycle were converged to within 1 × 10⁻³ and 1 × 10⁻⁵ au, respectively. Geometries were optimized to within 1 × 10⁻³ au. Triple- ζ basis sets were employed for all atoms. The core electrons up to and including the 4p, 5p, 2p, and 1s shells were frozen for molybdenum, tungsten, phosphorus, and oxygen atoms, respectively. Scalar relativistic corrections were explicitly included via the frozen-core potential. Relativistic corrections, along with spin state and geometry optimizations, were required for reliable predictions of structure and energetics. These calculations were conducted on an IBM SP2 system using the Amsterdam density functional codes.

In this work, small metal oxide clusters, as well as the complete Keggin unit, were used to determine proton affinity. The cluster approach has proven to be quite valuable for quantum chemical analyses of metals, metal-oxide, and metal sulfide systems provided that both the geometries and electronic structures were properly described. For metal oxides, in particular, the approximation of the surface and bulk by cluster calculations is very effective due to the relatively large gap between the highest and lowest occupied molecular orbitals. Weber⁵⁷ and Hoffmann,⁵⁸ for example, have reported similar energetics for both small and large clusters of metal oxides. The application of the cluster approach to calculations on the Keggin structure, however, is complicated by the three protons that are required to balance the charge. To emulate the charge on the Keggin unit, a negative charge must be added to the small metal oxide clusters. It is not at all clear how large the negative charge should be since the clusters are fractional representations of the Keggin structure. In addition, delocalization of charge over small clusters may affect calculated energies. Unlike bulk metal oxides, the role of cluster size is

TABLE 1: Characterization of Heteropolyacid Catalysts

sample	physisorbed + hydration per KU ^a	protonic water per KU ^b	protons per KU ^c	BET surface area ^d (m ² g ⁻¹)			
				373 K	473 K	573 K	673 K
PW	20.2	1.5	3.0	8	7	5	12
PMo	14.5	1.4	2.8	10	7	3	2
SiW	14	1.8	3.6	6	6	5	17
SiMo	10.4	1.8	3.6	7	5	7	18
Cs ₂	5.5	0.35	0.7				67

^a Water evolved at low temperature (less than 550 K). ^b Water loss from decomposition of Keggin unit. ^c Protons per Keggin unit calculated as 2 times the amount of evolved protonic water. ^d BET surface area measured after various pretreatment temperatures.

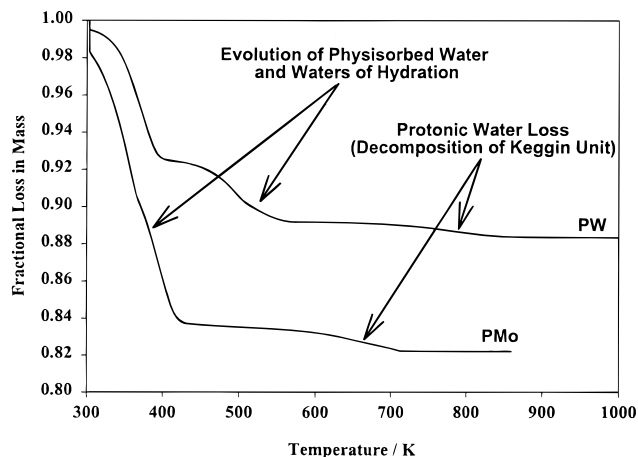


Figure 2. Thermal gravimetric analysis of phosphotungstic (PW) and phosphomolybdic (PMo) acids. Heating rate 10 K min⁻¹ in helium flowing at 100 cm³ min⁻¹. Mass of PW = 436.4 mg, and mass of PMo = 203.8 mg.

likely to be quite important. Therefore, to analyze these effects, we examined a series of different cluster sizes.

Results

Table 1 summarizes the results from thermal gravimetric analysis and dinitrogen adsorption. The surface areas of the materials were very low in all cases, typically less than 10 m² g⁻¹. During thermal gravimetric analysis, waters of hydration evolved first, leaving anhydrous Keggin units with associated protons. According to the results in Table 1, the HPA's in this study contained many waters of hydration. As the temperature continued to increase, "protonic water" evolved. This water is formed by extraction of an oxygen atom from the Keggin anion by two protons, thus decomposing the heteropolyacid. The number of these acidic protons per Keggin unit is also shown in Table 1. As anticipated from the stoichiometry, the heteropolyacids with phosphorus had approximately three protons per Keggin unit whereas those with silicon had about four protons per Keggin unit. Figure 2 shows the thermal gravimetric analysis for phosphomolybdic and phosphotungstic acids. Results from characterization of the cesium salt of phosphotungstic acid (Cs₂) are reported in Table 1 for comparison. The number of protons decreased and the surface area increased with partial substitution of cesium cations in the heteropolyacid.¹⁹

Figure 3 compares the rates of 1-butene double-bond isomerization over PMo and PW at 348 K and 20 min time on stream as a function of pretreatment temperature. Regardless of pretreatment condition, PW was much more active than PMo for butene isomerization. Interestingly, the specific rate of reaction over PW decreased significantly with increasing pretreatment temperature.

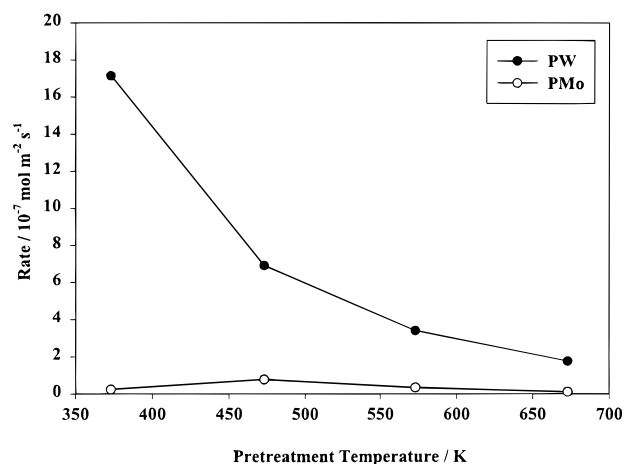


Figure 3. Effects of pretreatment conditions and addenda atoms on the rate of 1-butene isomerization. Temperature of reaction 348 K, 5 vol % butene in helium, 30 mL min⁻¹ total flow. Data taken at 20 min time on stream.

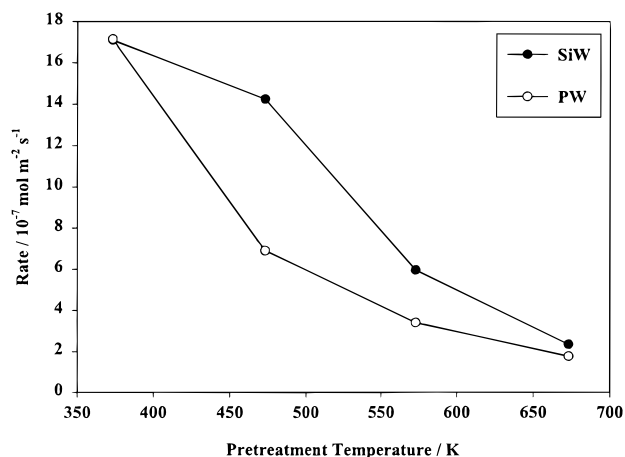


Figure 4. Effect of central atom on rate of 1-butene isomerization at various pretreatment conditions. Temperature of reaction 348 K, 5 vol % butene in helium, 30 mL min⁻¹ total flow. Data taken at 20 min time on stream.

Figure 4 illustrates the effect of central atom type on the rate of 1-butene isomerization over tungsten-based heteropolyacids. Clearly, the central atom was not as important as the addenda atom. Silicotungstic acid was slightly more active than phosphotungstic acid since the silicon-containing sample had a slightly higher acid site density. However, the trend of decreasing activity with increasing pretreatment temperature was also seen with SiW. Low pretreatment temperatures are apparently beneficial for this particular acid-catalyzed reaction.

The double-bond isomerization of *cis*-2-butene was also performed over the various catalysts, and the results are summarized in Table 2. As expected, the tungsten-based heteropolyacids were the most active. The product ratio of *trans*-2-butene to 1-butene, measured at similar conversion levels, was significantly higher over the tungsten-based materials.

Results from ammonia sorption microcalorimetry on the various catalysts are given in Figures 5–7. Figure 5 illustrates the similarity in heats of ammonia sorption on Cs₂ and PW, even though the total uptake was much lower on the Cs₂ sample. The low uptake of ammonia was due to the partial replacement of acidic protons with Cs ions. Also, the heat of ammonia sorption on PW was fairly constant with ammonia loading until all of the acid sites were titrated.

The effect of pretreatment conditions on the heats of ammonia sorption was also investigated. As shown in Figure 6, the PW

TABLE 2: Reaction Rate and Selectivity from *cis*-2-Butene Isomerization^a

sample	reaction rate		conversion (%)	product ratio ^b
	10 ⁻⁷ mol m ⁻² s ⁻¹	10 ⁻⁷ mol g ⁻¹ s ⁻¹		
PW	5.4	37.8	3.0	4.0
PMo	0.083	0.58	2.1	1.8
SiW	12.0	72.0	4.8	5.6
SiMo	0.33	1.7	4.0	2.4

^a Data at 20 min on stream, $T = 348$ K, 5 vol % C₄ = in He. ^b Ratio of *trans*-2-butene to 1-butene.

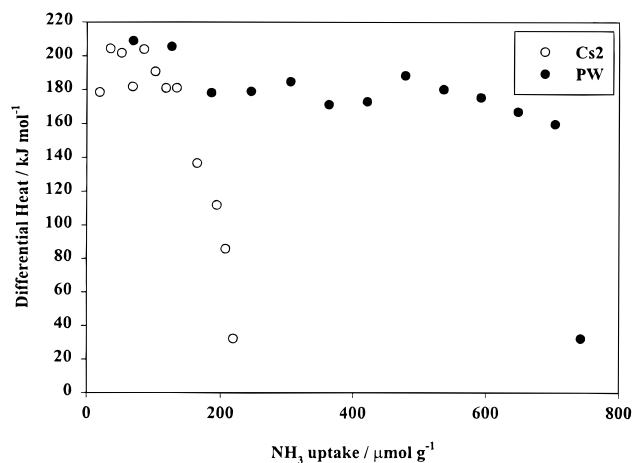


Figure 5. Comparison of the heats of ammonia sorption at 373 K for Cs₂ and PW pretreated at 473 K.

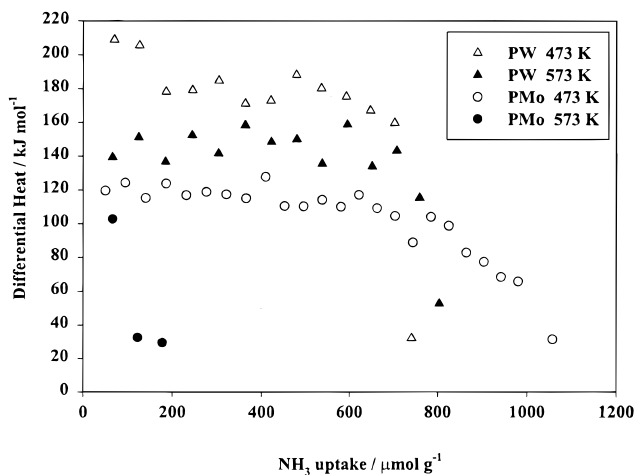


Figure 6. Comparison of the heats of ammonia sorption at 373 K for PW and PMo pretreated at 473 and 573 K.

sample pretreated at 473 K had higher heats of ammonia sorption (~30–50 kJ mol⁻¹) than did the same sample pretreated at 573 K. Figure 6 also compares of the heats of ammonia sorption over PW and PMo. For samples pretreated at 473 K, the heat of ammonia sorption was about 70 kJ mol⁻¹ higher on PW than on PMo. The PMo sample evidently decomposed after treatment at 573 K since the total uptake decreased dramatically.

Figure 7 shows relatively small differences in the heat of ammonia sorption for PW and SiW. However, after pretreatment at 473 K, PW had a slightly higher heat of ammonia sorption. The SiW sample had a greater uptake of ammonia since SiW has a greater proton density, as discussed earlier.

Results from the catalytic probe reactions clearly showed the tungsten-based heteropolyacids were more active than their

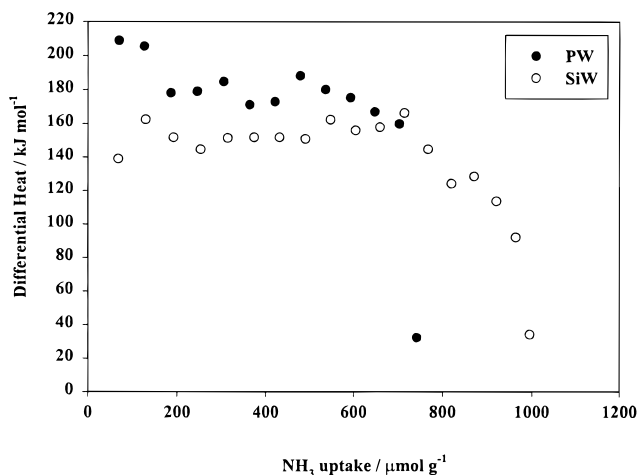


Figure 7. Effect of central atom on the heats of ammonia sorption at 373 K after pretreatment at 473 K.

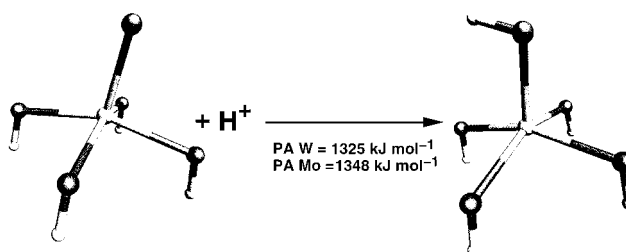


Figure 8. Proton affinity of the monomer cluster, MO₅.

molybdenum counterparts. The tungsten-containing HPA's also had higher ratios of *trans*-2-butene to 1-butene in the product stream from *cis*-2-butene reaction than the molybdenum HPA's. Microcalorimetry experiments measuring the heat of ammonia sorption on the various catalysts showed tungsten heteropolyacids evolved more heat when titrated with ammonia than molybdenum heteropolyacids. These experimental findings were then complemented with quantum chemical calculations.

A small metal oxide cluster containing one transition-metal atom was used as an initial model of the Keggin unit for the quantum chemical studies. Figure 8 shows the structure of this monomer cluster. The proton affinities of the W and Mo monomer clusters were 1325 and 1348 kJ mol⁻¹, respectively, indicating the proton is more strongly bound to the Mo cluster.

A metal oxide dimer was used to determine the optimal position of the acidic proton since a dimer is the smallest structural unit that contains terminal and bridging oxygen atoms. The proton affinities of the terminal and bridging oxygen atoms in W and Mo dimers are presented in Figure 9. For both metal oxide dimers, the proton affinity was significantly greater on the bridging oxygen compared to the terminal one, indicating the bridging site was the most favorable. In addition, the proton affinity of the bridging site on the W dimer was less than that of the same site on the Mo dimer. Analogous calculations were conducted on a trimer metal oxide cluster containing three transition-metal atoms and the central atom. As shown in Figure 10, the bridging site was favored over the terminal site by 370 kJ mol⁻¹. Again, the proton affinity for the W trimer was significantly lower than that for the Mo trimer. In addition to comparing the proton affinity of the terminal and bridge sites on the dimer and trimer models, the proton affinity of the terminal and bridge sites were compared on the tetramer cluster shown in Figure 11a. The proton affinity of the tungsten tetramer terminal site was 873 kJ mol⁻¹, about 300 kJ mol⁻¹ lower than the bridge site.

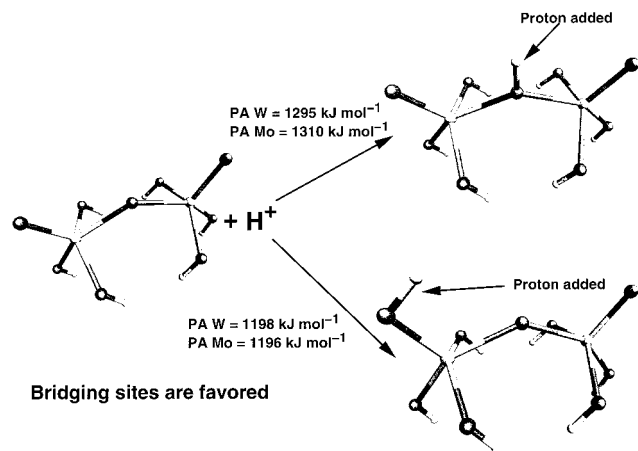


Figure 9. Calculation of proton position using the dimer cluster. PA W and PA Mo are the proton affinities of the tungsten and molybdenum clusters, respectively.

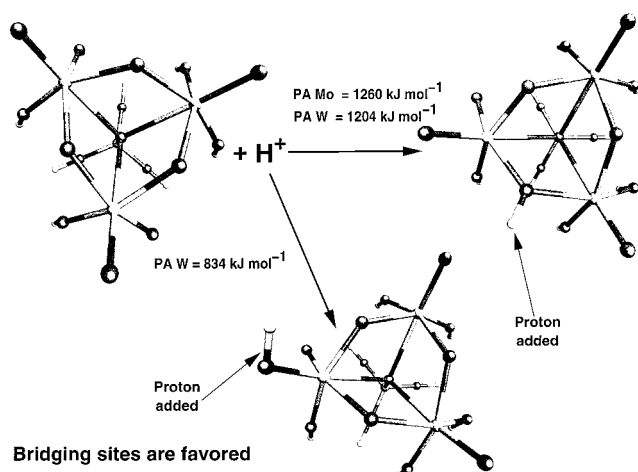


Figure 10. Determination of the proton position on the tungsten trimer cluster and a comparison of the PA W and PA Mo for the bridging position.

The small cluster calculations indicated the proton resides on the bridge site of the heteropolyacid. However, the Keggin structure has two inequivalent bridging oxygen atoms. Figure 11a shows a tetramer oxide cluster containing both types of bridging oxygen sites. The calculated proton affinity for each site was nearly the same (Figure 11b), within the error of the DFT method.

As seen in Table 3, the size of the negatively charged metal oxide cluster greatly affects the calculated proton affinity. Thus, calculations were also conducted on a full Keggin unit to eliminate the cluster size effect. Prior to calculating the proton affinity, Keggin units with a phosphorus central atom were completely geometry optimized. Table 4 presents a comparison of the bond distances obtained from the DFT calculations to those determined experimentally. The bonds listed in Table 4 correspond the labels in Figure 1. Clearly, the bond distances derived from DFT were in excellent agreement with experiment. For the calculation of proton affinity, two protons were placed on the Keggin anion to give the entire starting structure a charge of -1 . The affinity of the anion for the third proton was then calculated based on the energies of the structures depicted in Figure 12. Full geometry optimization of the molybdenum and tungsten Keggin units resulted in proton affinities of 1126 and 1088 kJ mol^{-1} , respectively. The proton affinity of the Keggin unit containing tungsten was 38 kJ mol^{-1} lower than that containing molybdenum, which is consistent with the trends

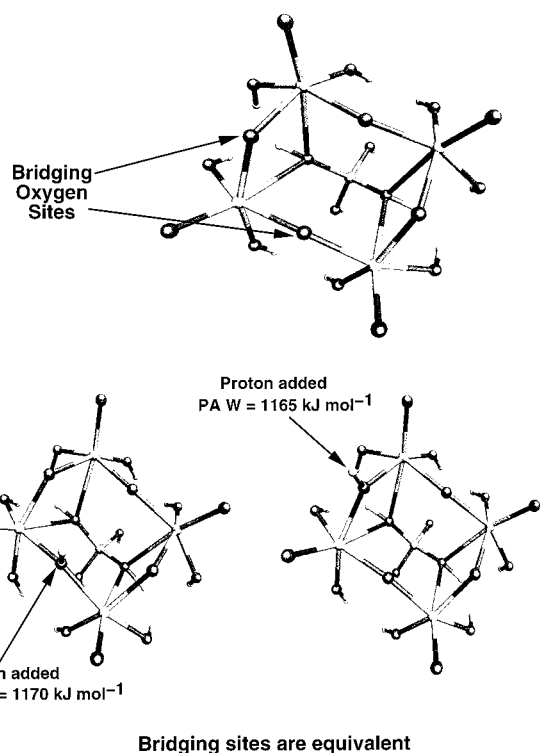


Figure 11. (a) Tetramer cluster used to compare the proton affinity of the two bridging sites. (b) Proton affinities of the W tetramer cluster calculated on the two bridging sites.

TABLE 3: Effect of Addenda Atoms on Proton Affinities of Metal Oxide Clusters

cluster	proton affinity (kJ mol^{-1})	
	tungsten	molybdenum
monomer	1325	1348
dimer	1295	1310
trimer	1204	1260
tetramer	1165	1195
Keggin unit	1088	1126

TABLE 4: Structural Optimization of the Keggin Unit

bond	tungsten (\AA)		molybdenum (\AA)	
	experiment ^a	DFT	experiment ^b	DFT
M=O	1.71	1.76	1.66	1.71
M-O-M 1	1.90	1.98	1.96	1.95
M-O-M 2	1.91	1.98	1.97	1.96
M-O _c	2.44	2.51	2.43	2.45
P-O	1.53	1.58	1.53	1.53

^a Reference 76. ^b Reference 39.

observed with the small clusters. While the relative proton affinities across a single-cluster size show the same trends (Table 3), the absolute values are much higher on the smaller clusters. The proton affinities for the tungsten HPA on the monomer, dimer, trimer, tetramer, and full Keggin structures were 1325, 1295, 1204, 1165, and 1088, respectively. The negative charge on the cluster is more delocalized over the larger systems.

Discussion

As discussed in the Introduction, no single technique provides unambiguous information regarding the strong acidity of solids important for catalysis. Therefore, a combination of experimental methods and quantum chemical calculations was used to study the well-known Keggin-type heteropolyacids.

Double-bond isomerization of butene has long been used as a catalytic probe of surface acidity.⁵⁹⁻⁶¹ The large effect of the

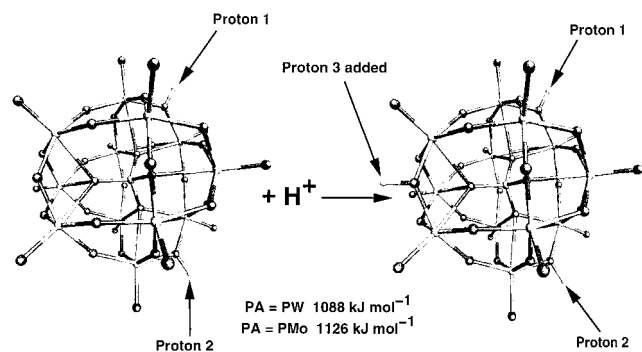


Figure 12. The Keggin unit used for the calculation of proton affinity.

addenda atoms on the rates of 1-butene and *cis*-2-butene isomerization, as illustrated in Figure 3 and Table 2, is entirely consistent with the general recognition that heteropolyacids based on W are more acidic than those based on Mo. Since the surfaces of the catalysts are probably covered with hydrocarbon species during reaction, it is actually quite interesting that differences in acid strength between the materials are not leveled completely. Additional evidence for the differences in acid strength is derived from the product distribution in the *cis*-2-butene reaction. Differences in the ratio of *trans*-2-butene to 1-butene and catalyst acidity have been observed over various solid acids.^{60–63} Higher *trans*-butene/1-butene ratios were associated with stronger solid acids. Misono et al. speculated that the selective formation of one isomer over the other was due to differences in the energy barrier for their formation.⁶³ Nevertheless, the product ratio has been claimed to be an indicator of acid strength.³ At similar levels of conversion, the *trans*-2-butene/1-butene ratios of the W-based heteropolyacids were about a factor of 2 greater than those of Mo-based catalysts, which is consistent with the ranking of acid strength based on catalyst activity.

Water appears to play a critical role in the acidity of the heteropolyacid. For example, the activity of the W-based catalysts for butene isomerization decreased significantly (Figure 4) with increasing pretreatment temperature, presumably due to the loss of water from the samples. Destruction of the Keggin unit may also account for the low activity at a pretreatment temperature of 673 K. Matsuda et al. also explored the effect of pretreatment on the activity of heteropolyacids for butene isomerization.⁶⁴ Similar to our results, conversion of butene was lower at higher pretreatment temperatures. In addition, the product stream from catalysts hydrated with D₂O contained doubly labeled butenes, indicating that water molecules associated with the heteropolyacid can be involved the formation of the acid site. Kim et al. also showed injection of water into the feed increased the activity of phosphomolybdic acid for both 1-butene and *cis*-2-butene isomerization reactions.⁶⁵

When waters of hydration are present in the heteropolyacids, acidic protons are associated with H₃O₂⁺ bridges. These acidic protons are very mobile in the solid, as demonstrated by the high ion conductivities of hydrated heteropolyacids.⁶⁶ As shown in Table 1, our as-received samples contained large amounts of water, the majority of which evolves at temperatures lower than 550 K. Therefore, we attribute the variations in activity with pretreatment temperature to the different water contents of the samples. Dumesic et al. have also shown that water is critical to the alkane isomerization activity of sulfated zirconia, another strongly acidic solid.^{67,68} Due to the complicating effect of water on the catalytic activity of solid acids, we also pursued ammonia sorption microcalorimetry as a characterization tool.

The polar molecule ammonia not only adsorbs on the external surface of the heteropolyacid but also penetrates into the secondary structure to form an ammonium salt. The heat evolved in this process is virtually the enthalpy of ammonium salt formation since nearly all of the acidic protons are located in the bulk of the solids. For this measurement to have any relevance to surface acidity, ammonia sorption on a high surface area material is needed for comparison.

Partially substituted cesium salts of heteropolyacids are very active, strongly acidic solid catalysts.⁶⁹ In an earlier study, we synthesized Cs₂HPW₁₂O₄₀ (Cs₂) and verified its high activity for butane and pentane skeletal isomerizations as well as 1-butene double-bond isomerization.¹⁹ The important property of this material for the current work is its relatively high specific surface area. From simple geometric arguments, the anticipated percentage of protons on the external surface is about 30%. By comparing the heats of ammonia sorption on PW (very few exposed acidic protons) to the heats of sorption on Cs₂ (larger fraction of exposed protons), the effects of adsorption versus absorption on ΔH can be determined. As shown in Figure 5, the heats of ammonia sorption were about $190 \pm 15 \text{ kJ mol}^{-1}$ on both samples, indicating the heats of ammonia adsorption and absorption are similar. The total ammonia uptake was lower on the Cs₂ sample since two of the acidic protons have been replaced by cesium cations. Results of this experiment enable the use of ammonia sorption microcalorimetry, which probes mainly bulk acid sites, to derive information on the acid character of the surface.

Ranking of solids with different chemical structures using ammonia sorption microcalorimetry is fraught with difficulty due to the complex interactions of the ammonia with the adsorbent. In this work, however, structurally similar compounds were examined. All samples were Keggin-type heteropolyacids. As shown in Figure 6, the heats of ammonia sorption were lower for PMo than PW, regardless of pretreatment temperature, and these results are consistent with the acidity ranking derived from catalytic experiments.

The effect of pretreatment temperature on the acidity of the heteropolyacid is also evident from the microcalorimetry results. For a pretreatment temperature of 473 K, ΔH_{sorp} on PW was approximately 190 kJ mol^{-1} , but when the pretreatment temperature was increased to 573 K, ΔH_{sorp} dropped to nearly 150 kJ mol^{-1} . Jozefowicz et al. obtained values of approximately 180 kJ mol^{-1} for an activation temperature of 323 K and 150 kJ mol^{-1} for activation at 523 K⁷⁰ on a similar sample. Kapustin et al. found comparable values as well.⁷¹ Jozefowicz et al. attribute the increased heats of ammonia sorption at lower temperatures to an inductive effect of water on the acid strength of the proton.⁷⁰ It is possible, however, that the increase in ΔH_{sorp} at lower pretreatment temperatures was due to the solvation of ammonia. Assuming the process of forming the ammonium salt of PW was similar in the hydrated and anhydrous condition, only the solvation of ammonia in the waters of crystallization would be an additional step in the sorption process. The heat of solution of gaseous ammonia in water is approximately 34 kJ mol^{-1} ,⁷² which would account for the increase from 150 kJ mol^{-1} in the dehydrated state to 190 kJ mol^{-1} in the hydrated state.

Many microcalorimetric studies have been conducted using ammonia as a probe molecule for acidic zeolites. For ammonia adsorption in dehydrated H-ZSM-5, H-ZSM-12, and H-Y, ΔH_{ads} is about 150 kJ mol^{-1} ,^{11,15,49} which is similar to results on dehydrated PW reported here.

The effect of the central atom on the acidity of a given

heteropolyacid was also studied and found to be insignificant. Little difference was observed in the heats of ammonia sorption for PW and SiW, which is in agreement with solution-phase acidity measurements.⁷³ Similar results were found for the molybdenum-based heteropolyacids. No clear difference was seen between SiW and PW in the catalytic studies as well. The rates of 1-butene isomerization were comparable for both samples, and the *trans*-2-butene/1-butene product ratios from *cis*-2-butene isomerization were similar.

The final phase of this work involved quantum chemical calculations of model heteropolyacids. As a first step, the proton affinity was used to deduce a ranking of acid strength. This approach is not strictly justified because acid properties are also dependent on the protonation of a basic molecule. Nevertheless, since the materials in this study are structurally similar, proton affinity should provide a consistent ranking. Indeed, much work has already been conducted on determining the proton affinities of zeolites,^{9,32,35,36,74,75} and ranking of heteropolyacid strength according to proton affinity seems to be a logical extension.

The heteropolyacids studied here possess a uniquely defined Keggin unit which is tractable computationally and solvable without termination effects. However, small, representative metal oxide clusters were used to determine the most energetically favorable position of the acidic proton. In the presence of water, the acidic proton resides in $H_5O_2^+$ bridges, as discussed earlier. The position of the proton on the anhydrous heteropolyacid is less clear. Results from our quantum chemical calculations indicate the lowest energy site is a bridging oxygen atom. Another possibility is that the acidic proton is stabilized on a terminal oxygen by hydrogen bonding to a neighboring Keggin ion. However, the difference in affinity between a proton residing on a terminal and on a bridge oxygen is calculated to be about 300 kJ mol⁻¹ for the tetramer cluster, which is the best cluster representation of the Keggin unit that we investigated. Since typical energies associated with hydrogen bonds are only 60 kJ mol⁻¹,¹⁰ we believe that hydrogen bonding is not adequate to stabilize the acidic proton on the terminal oxygen of anhydrous heteropolyacids. In the Keggin unit, there exist two inequivalent bridging oxygen atoms defined by their relationship to the central oxygen atoms. Our calculations on a small tetramer cluster indicated the two different bridge sites were equivalent with respect to proton affinity.

Once the energetically favorable location of the proton was determined, we explored the effects of addenda atoms and cluster size on proton affinity. As shown in Table 3, the tungsten-based clusters always had lower proton affinities than their corresponding molybdenum-based clusters. This result is consistent with the conclusion derived from experiments that tungsten heteropolyacids are stronger acids. Table 3 also reveals a rather strong cluster size effect in the calculation of proton affinity. This effect is due to the difficulty in assigning charge to the small clusters. In each case, the cluster was assigned a -1 charge before the addition of a proton. Since the small clusters have very few atoms over which to distribute the negative charge, the interactions of these clusters with a proton are expected to be greater due to simple electrostatic attraction. These results necessitated the calculation of a full Keggin unit to derive meaningful values of the proton affinity.

In the study of the full Keggin unit, complete structural optimization of the anion was performed. The match between experimental results and calculated bond distances in Table 4 is very good. Determination of proton affinity required the addition of two protons to the Keggin unit in order to give an anion with a -1 charge. Many computations are required to

determine the lowest energy positions of the protons with respect to one another on the Keggin unit, but that is beyond the scope of this work. Since the negative charge in the Keggin unit is well-dispersed,⁴¹ the likelihood of neighboring protons interacting with each other is small. For this reason, the two protons were placed at positions far from one another. The full Keggin structure was structurally optimized after placing two protons on the Keggin unit and again after addition of the third proton. These computations yielded the value of 1126 kJ mol⁻¹ for the proton affinity of the third binding site on the molybdenum Keggin unit. For the tungsten case, a value of 1088 kJ mol⁻¹ was determined. The difference of 38 kJ mol⁻¹ compares well to the values obtained from the small cluster calculations, indicating the cluster calculations may yield reasonable results for the differences among the heteropolyacids. However, calculations on the full Keggin units are needed for absolute energies. This point is illustrated in Table 3, where the proton affinities of the larger clusters converged to the value of the complete Keggin ions. Nevertheless, all calculations are consistent with an overall ranking of acid strength that places tungsten HPA higher than molybdenum HPA.

Conclusions

This study utilized a unique combination of experimental and theoretical methods to assess the acid strength of solid Keggin-type heteropolyacids. Results from butene isomerization, ammonia sorption microcalorimetry, and quantum chemical calculations indicated tungsten-based heteropolycompounds were stronger solid acids than molybdenum-based materials. However, the influence of the central atom (P versus Si) on acid strength was rather small. Residual waters of hydration in the solid state played a critical role in the acidity of the samples. For example, hydrated phosphotungstic acid had a greater catalytic activity and a higher heat of ammonia sorption than a dehydrated sample. The most energetically favorable site for the acidic proton in anhydrous heteropolyacids was determined by quantum chemical calculations to be a bridging oxygen atom. The calculated proton affinity was a strong function of the cluster size of model metal oxides due to difficulties in assigning charge. Therefore, proton affinity was determined on a full Keggin unit. The proton affinities of structurally optimized Keggin units were completely consistent with acidity rankings derived from experiments on solid- and solution-phase heteropolyacids.

Acknowledgment. We gratefully acknowledge a grant from the National Science Foundation in Environmentally Conscious Chemical Manufacturing (Grant No. GER9452654). Additional funding for this work was also provided by the Virginia Academic Enhancement Program. We would like to thank Mr. P. S. Venkataraman for his initial work on DFT calculations of the entire Keggin structure.

References and Notes

- (1) Council, N. R. *Catalysis Looks to the Future*; National Academy Press: Washington, DC, 1992.
- (2) Corma, A. *Chem. Rev.* **1995**, *95*, 559.
- (3) Tanabe, K.; Misono, M.; Ono, Y.; Hattori, H. *New Solid Acids and Bases*; Elsevier: Kodansha, Tokyo, 1989; Vol. 51.
- (4) Misono, M.; Okuhara, T. *CHEMTECH* **1993**, *23*, 23.
- (5) Hattori, H.; Takahashi, O.; Takagi, M.; Tanabe, K. *J. Catal.* **1981**, *68*, 132.
- (6) Arata, K. *Adv. Catal.* **1990**, *37*, 165.
- (7) Cheung, T. K.; Gates, B. C. *CHEMTECH* **1997**, *27*, 28.
- (8) Farneth, W. E.; Gorte, R. J. *Chem. Rev.* **1995**, *95*, 615.
- (9) Sauer, J. *Chem. Rev.* **1989**, *89*, 199.
- (10) Van Santen, R. A.; Kramer, G. J. *Chem. Rev.* **1995**, *95*, 637.

- (11) Lee, C.; Parrillo, D. J.; Gorte, R. J.; Farneth, W. E. *J. Am. Chem. Soc.* **1996**, *118*, 3262.
- (12) Umansky, B.; Engelhardt, J.; Hall, W. K. *J. Catal.* **1991**, *127*, 128.
- (13) Lefebvre, F.; Liu-Cai, F. X.; Auroux, A. *J. Mater. Chem.* **1994**, *4*, 125.
- (14) Parrillo, D. J.; Gorte, R. J. *J. Phys. Chem.* **1993**, *97*, 8786.
- (15) Parrillo, D. J.; Lee, C.; Gorte, R. J. *Appl. Catal., A* **1994**, *110*, 67.
- (16) Tabora, J. E.; Davis, R. J. *J. Am. Chem. Soc.* **1996**, *118*, 12240.
- (17) Sommer, J.; Hachoumy M.; Garin, F. *J. Am. Chem. Soc.* **1995**, *117*, 1135.
- (18) Tabora, J. E.; Davis, R. J. *J. Catal.* **1996**, *162*, 125.
- (19) Bardin, B. B.; Davis, R. J. *Top. Catal.* **1998**, *6*, 77.
- (20) Liu, H.; Lei, G. D.; Sachtler, W. M. H. *App. Catal. A: Gen.* **1996**, *137*, 167.
- (21) Haw, J. F.; Xu, T. *Adv. Catal.* **1998**, *42*, 115.
- (22) Haw, J. F.; Nicholas, J. B. *Stud. Surf. Sci. Catal.* **1996**, *101A*, 573.
- (23) Heeribout, L.; Semmer, V.; Batamack, P.; Doremieux-Morin, C.; Vincent, R.; Fraissard, J. *Stud. Surf. Sci. Catal.* **1996**, *101B*, 831.
- (24) Biaglow, A. I.; Gorte, R. J.; Kokotailo, G. T.; White, D. *J. Catal.* **1994**, *148*, 779.
- (25) Keister, J. W.; Riley, J. S.; Baer, T. *J. Am. Chem. Soc.* **1993**, *115*, 12613.
- (26) Bobette, D. N.; Cooks, R. G. *Int. J. Mass Spectrom. Ion Phys.* **1991**, *106*, 249.
- (27) Martin, J. M. L.; Lee, T. J. *Chem. Phys. Lett.* **1996**, *258*, 136.
- (28) Gale, J. D. *Top. Catal.* **1996**, *3*, 169.
- (29) Adachi, M.; Contescu, C.; Schwarz, J. A. *J. Catal.* **1996**, *158*, 411.
- (30) Contescu, C.; Popa, V. T.; Miller, J. B.; Ko, E. I.; Schwarz, J. A. *J. Catal.* **1995**, *157*, 244.
- (31) Contescu, C.; Jagiello, J.; Schwarz, J. A. *Langmuir* **1993**, *9*, 1754.
- (32) Kramer, G. J.; Van Santen, R. A. *J. Am. Chem. Soc.* **1993**, *115*, 2887.
- (33) Chandra, A. K.; Goursot, A.; Fajula, F. *J. Mol. Catal. A: Chem.* **1997**, *119*, 45.
- (34) Bates, S.; Dwyer, J. *J. Mol. Struct.* **1994**, *306*, 57.
- (35) Gonzales, N. O.; Bell, A. T.; Chakraborty, A. K. *J. Phys. Chem. B* **1997**, *101*, 10058.
- (36) Eichler, U.; Braendle, M.; Sauer, J. *J. Phys. Chem. B* **1997**, *101*, 10035.
- (37) *Chem. Rev.* Hill, C. L., Ed.; **1998**, 98.
- (38) Misono, M. *Catal. Rev.-Sci. Eng.* **1987**, *30*, 269.
- (39) Okuhara, T.; Mizuno, N.; Misono, M. *Adv. Catal.* **1996**, *41*, 113.
- (40) Jansen, R. J. J.; van Veldhuizen, H. M.; Schwegler, M. A.; van Bekkum, H. *Recl. Trav. Chim. Pays-Bas* **1994**, *113*, 115.
- (41) Pope, M. T. *Heteropoly and Isopoly Oxometalates*; Springer-Verlag: Berlin, 1983.
- (42) Kozhevnikov, I. V. *Catal. Lett.* **1995**, *34*, 213.
- (43) Kozhevnikov, I. V. *Russ. Chem. Rev.* **1987**, *56*, 1417.
- (44) Lee, K. Y.; Mizuno, N.; Okuhara, T.; Misono, M. *Bull. Chem. Soc. Jpn.* **1989**, *62*, 1731.
- (45) Barrows, J. N.; Jameson, G. B.; Pope, M. T. *J. Am. Chem. Soc.* **1985**, *107*, 1771.
- (46) Moffat, J. B. *J. Mol. Catal.* **1984**, *26*, 385.
- (47) Tatematsu, S.; Hibi, T.; Okuhara, T.; Misono, M. *Chem. Lett.* **1984**, 865.
- (48) Essayem, N.; Coudurier, G.; Fournier, M.; Vedrine, J. C. *Catal. Lett.* **1995**, *34*, 223.
- (49) Parrillo, D. J.; Gorte, R. J. *Catal. Lett.* **1992**, *16*, 17.
- (50) Bordawekar, S. V.; Doskocil, E. J.; Davis, R. J. *Langmuir* **1998**, *14*, 1734.
- (51) Neurock, M. *Appl. Catal. A: Gen.* **1997**, *160*, 169.
- (52) Ziegler, T. *Chem. Rev.* **1991**, *91*, 651.
- (53) Vosko, S. H.; Wilk, L.; Nusair, M. *Can. J. Phys.* **1980**, *58*, 1200.
- (54) Becke, A. D. *Phys. Rev. A* **1988**, *38*, 3098.
- (55) Becke, A. D. *ACS Symp. Ser.* **1989**, *394*, 165.
- (56) Perdew, J. P. *Phys. Rev. B* **1986**, *33*, 8822.
- (57) Weber, R. S. *J. Phys. Chem.* **1994**, *98*, 2999.
- (58) Schiott, B.; Jorgensen, K. A.; Hoffmann, R. *J. Phys. Chem.* **1991**, *95*, 2297.
- (59) Lucchesi, P. J.; Baeder, D. L.; Longwell, J. P. *J. Am. Chem. Soc.* **1959**, *81*, 3235.
- (60) Hightower, J. W.; Hall, W. K. *J. Am. Chem. Soc.* **1967**, *89*, 778.
- (61) Hightower, J. W.; Hall, W. K. *J. Phys. Chem.* **1967**, *71*, 1014.
- (62) Aguayo, A. T.; Arandes, J. M.; Olazar, M.; Bilbao, J. *Ind. Eng. Chem. Res.* **1990**, *29*, 1172.
- (63) Misono, M.; Yoneda, Y. *J. Phys. Chem.* **1972**, *76*, 44.
- (64) Matsuda, T.; Sato, M.; Kanno, T.; Miura, H.; Sugiyama, K. *Faraday Trans.* **1981**, *1*, 3107.
- (65) Kim, J. J.; Lee, W. Y.; Rhee, H. K. *Chem. Eng. Commun.* **1985**, *34*, 49.
- (66) Colombari, P. *Proton conductors: solids, membranes, and gels—materials and devices*; Cambridge, University Press: Cambridge, 1992.
- (67) Kobe, J. M.; Gonzalez, M. R.; Fogash, K. B.; Dumesic, J. A. *J. Catal.* **1996**, *164*, 459.
- (68) Gonzalez, M. R.; Kobe, J. M.; Fogash, K. B.; Dumesic, J. A. *J. Catal.* **1996**, *160*, 290.
- (69) Na, K.; Okuhara, T.; Misono, M. *Faraday Trans.* **1995**, *91*, 367.
- (70) Jozefowicz, L. C.; Karge, H. G.; Vasilyeva, E.; Moffat, J. B. *Microporous Mater.* **1993**, *1*, 313.
- (71) Kapustin, G. I.; Brueva, T. R.; Klyachko, A. L.; Timofeeva, M. N.; Kulikov, S. M.; Kozhevnikov, I. V. *Kinet. Catal.* **1990**, *31*, 896.
- (72) *CRC Handbook of Chemistry and Physics*, 71st ed.; Lide, D. R., Ed.; CRC Press: Boston, 1990.
- (73) Polotebnova, N. A.; Kozlenko, A. A.; Furtune, L. A. *Russ. J. Inorg. Chem.* **1976**, *21*, 1511.
- (74) Mortier, W. J.; Sauer, J.; Lercher, J. A.; Noller, H. *J. Phys. Chem.* **1984**, *88*, 905.
- (75) Chandra, A. K.; Goursot, A.; Fajula, F. *J. Mol. Catal. A: Chem.* **1997**, *119*, 45.
- (76) Brown, G. M.; Noe-Spirlet, M. R.; Busing, W. R.; Levy, H. A. *Acta Crystallogr.* **1977**, *B33*, 1038–1046.